ATLAS NOTE

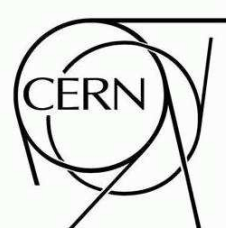

A Parameterization of the Energy Loss of Muons in the ATLAS Tracking Geometry

D. López Mateos[*,1,2], E. W. Hughes[1], A. Salzburger[3,4]

[1] *Columbia University, New York, NY 10027, USA*
[2] *California Institute of Technology, Pasadena, CA 91125, USA*
[3] *CERN, PH Department, CH-1211 Geneva 23, Switzerland*
[4] *Leopold-Franzens Universität, A-6020 Innsbruck, Austria*
[*] corresponding author (david.lopez@cern.ch)

Abstract

A parameterization of the muon energy loss in the ATLAS Calorimeters is presented. This parameterization is based on a GEANT4 simulation of the calorimeter absorber materials. The parameterization provides a calculation of the energy loss of muons in each calorimeter volume. This calculation has been integrated into the ATLAS Tracking Geometry to be used by tracking tools to improve the fit of candidate muon tracks traversing the calorimeters. The validation of this parameterization has been performed and compared to the ATLAS GEANT4 full simulation. Finally, possible uses of this parameterization as part of the tracking tools are discussed.

Contents

1 Introduction

Muons traverse the Inner Detector and the Calorimeters in their journey through the ATLAS detector before reaching the Muon Spectrometer. By the time they reach the entrance of the Muon Spectrometer, muons have penetrated through over 100 radiation lengths (X_0) of material. Relativistic muons going through matter lose energy mostly through electromagnetic processes: ionization, e^+e^- pair-production, and bremsstrahlung. Ionization energy losses have been studied in detail, and an expression of the mean energy loss per unit length as a function of muon momentum and material type exists in the form of the Bethe-Bloch equation [1]. However, muons in ATLAS will also lose a significant amount of energy through e^+e^- pair-production and bremsstrahlung and no closed-form formula exists for the mean energy loss from these processes. The cross-section for these processes is well understood, so GEANT4 can be used reliably to parameterize the associated energy loss. Understanding the energy loss is important for tracking algorithms, especially those performing combined fits that make use of Inner Detector and Muon Spectrometer hits.

In ATLAS, tracking algorithms are converging towards the use of common tracking tools [2] which provide all users with well-validated utilities for different tracking tasks such as track transport, track fitting, bremsstrahlung recovery, et cetera. The geometrical description used by these tools is encapsulated in a set of objects collectively known as the Tracking Geometry [3]. In this document a new parameterization of the energy loss of muons integrated in the Tracking Geometry is discussed and validated. The integration of the new parameterization required the development of new tracking tools that are described in Section 2. The rest of the document focuses on the new parameterization and the validation of the energy loss of muons traversing the Tracking Geometry.

2 Material Effects in the Tracking Geometry

When a muon traverses detector material, it undergoes successive deflections and a loss of energy due to mainly electromagnetic processes. In this document we are mostly interested in the energy loss and will not refer any further to these deflections or multiple scattering. These material effects need to be included in the transport of a track through the ATLAS detector by fitters and other applications using

the parameterization of the track. Their effect on muon momentum reconstruction can be significant for muons of energies up to a few hundred GeV.

Generally, material effects need to be applied to the track parameterization on one or several surfaces along the trajectory of the track. The details of how materials affect the parameterization of the track on each of these surfaces is described in [4]. In order to perform a correct energy loss correction on the chosen surfaces, an understanding of the material around them is necessary. The common tracking tools have a mechanism to map the material properties used in the GEANT4 full simulation to layers in the Tracking Geometry. These material maps allow analytic calculations of the energy loss of tracks crossing each layer using, for example, the Bethe-Bloch formula.

However, not all energy loss effects can be estimated from closed-form formulas that depend on the properties of the traversed material. In particular, GEANT4 parameterizations are necessary to estimate the energy loss of muons correctly (see Section 3). In order to allow more flexibility in the calculation of energy loss (and multiple scattering) tools inheriting from the interface `IMaterialEffectsOnTrackProvider` can be added to the volumes of the Tracking Geometry. These tools provide a set of `MaterialEffectsOnTrack` that encapsulate the material effects, otherwise provided by default by the static layers of the Tracking Geometry. One implementation of this interface exists for calculating energy loss surfaces for muons traversing the calorimeters. This implementation is called `Calo::MaterialEffectsOnTrackProvider`. The main features of this implementation are:

- It calculates the surfaces where the energy loss should be applied dynamically, so that no matter what the trajectory is inside the calorimeter, there is always an energy loss surface.
- It calculates the number of radiation lengths inside the calorimeter using information from the detector design.
- The final calculation of the energy loss is performed using an `IEnergyLossCalculator` which can be configured in the job steering.
- The measured energy deposit in the calorimeters can be passed to the `IEnergyLossCalculator`. This measured energy deposit is calculated through an `IEnergyDepositionTool` that can also be configured in the job steering.

The `Calo::MaterialEffectsOnTrackProvider` is part of the calorimeter active volumes in the Tracking Geometry and it can be used by an `Extrapolator` when appropriately configured. Figure 1 shows the Tracking Geometry volumes and the surfaces created by a `Calo::MaterialEffectsOnTrackProvider`. In this document an implementation of the `IEnergyLossCalculator` that contains a parameterization of the energy loss in the calorimeter volumes is discussed. This implementation can be found in the ATLAS CVS repository under the name `ParamEnergyLossCalculator`. This tool does not make use of the measured energy deposit, so this feature is not relevant in that context. However, a method that uses the measured energy deposit to estimate the energy loss which has been implemented as an `IEnergyLossCalculator` [5].

3 A Parameterization of Energy Loss in each Tracking Volume

The modular nature of the Tracking Geometry requires that energy loss is calculated and added to the track properly in each of its volumes. In this section, we discuss how this is done, considering the different characteristics of each volume.

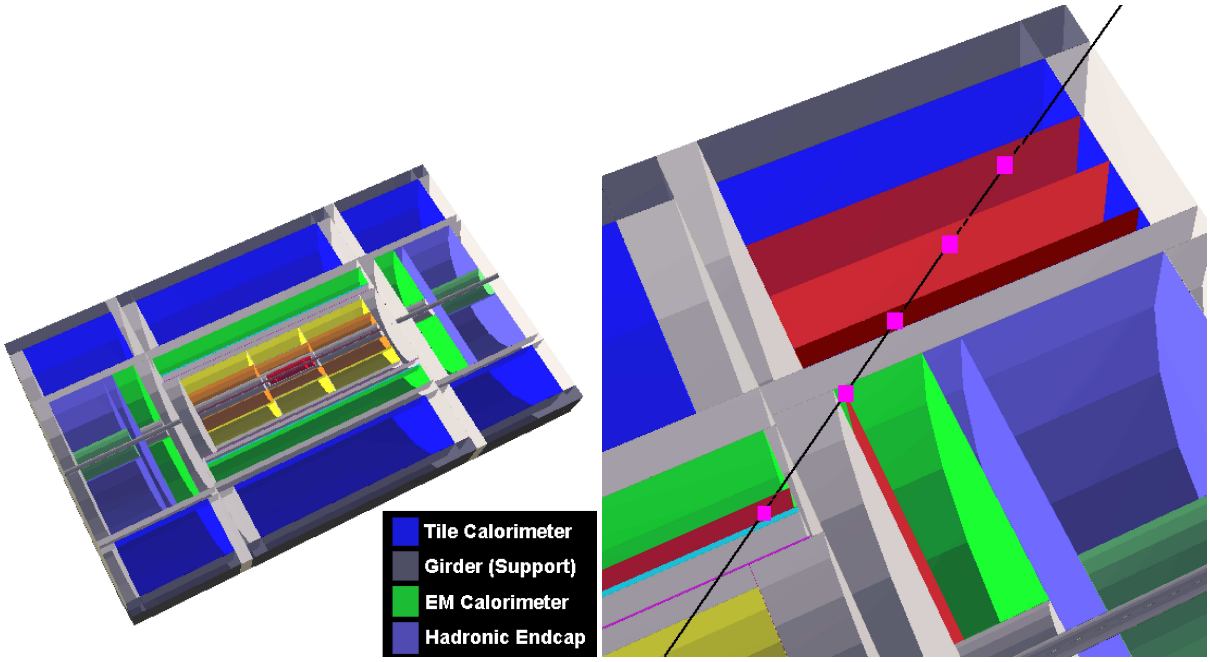

Figure 1: 3-D Visualization of the ATLAS ID and Calorimeters as volumes in the Tracking Geometry. Example material-update surfaces created by the `Calo::MaterialEffectsOnTrackProvider` when extrapolating a muon candidate through the calorimeters.

3.1 Parameterization of Energy Loss in the Absorbers

As already mentioned, the estimation of the energy loss of muons traversing ATLAS requires the use of parameterizations. In particular, obtaining a good estimate in the calorimeters is most important, since most of the energy loss occurs there. For simplicity, in this note the energy loss of muons in the calorimeters was estimated from the energy loss expected in the absorbers. Since some of the energy is also lost in the active media of the calorimeters, a correction for this is also performed (see Section 3.2).

In order to obtain a parameterization of the energy loss that is valid for any extrapolation inside ATLAS, it was necessary to provide this parameterization as a function of both the muon momentum and the thickness of the material traversed. Muons of 19 different momenta in the range 5 to 1000 GeV were simulated passing through blocks of material with 5 different thicknesses. The process was repeated for three different materials: lead, copper and iron, corresponding to the absorber materials for the EM calorimeters, the Hadronic Endcap calorimeter and the Tile calorimeter, respectively. For each data sample 2000 muons were simulated. The energy loss distributions were then fit to Landau distributions and the defining parameters of these Landau distributions were parameterized:

- Most probable value $= E_{\rm loss}^{\rm mpv} = E_{\rm loss}^{\rm mpv}(p_\mu, x)$.
- Width parameter (see the Appendix for the precise definition) $= E_{\rm loss}^{\sigma} = E_{\rm loss}^{\sigma}(p_\mu, x)$,

where x is the material thickness in radiation lengths, X_0. The parameters were fit first as a function of x for fixed momenta. Both $E_{\rm loss}^{\rm mpv}(x)$ and $E_{\rm loss}^{\sigma}(x)$ were well described by the function $a_0 x + a_1 x \ln(x/X_0)$ at fixed momenta. Figures 2 and 3 illustrate these fits for 5 GeV and 1 TeV muons, respectively, and the three materials considered. In order to complete the parameterization as a function of p_μ and x, the a_i parameters were fitted as a function of p_μ. The following function sufficed to obtain satisfactory fits:

$$a_i = b_{i,0} + b_{i,1} \ln B p_\mu + b_{i,2} p_\mu, \tag{1}$$

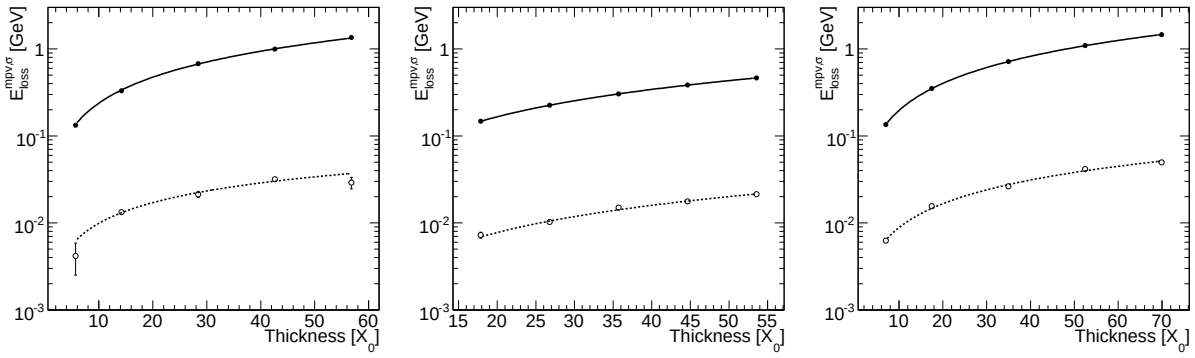

Figure 2: Parameterization of the Landau distribution parameters as a function of thickness of material traversed for 5 GeV muons in iron (left), lead (center) and copper (right). The fitting functions were $a_0x + a_1x\ln(x/X_0)$. The solid (empty) circles and solid (dashed) line correspond to the data and fitted functions for $E_{\rm loss}^{\rm mpv}$ ($E_{\rm loss}^{\sigma}$).

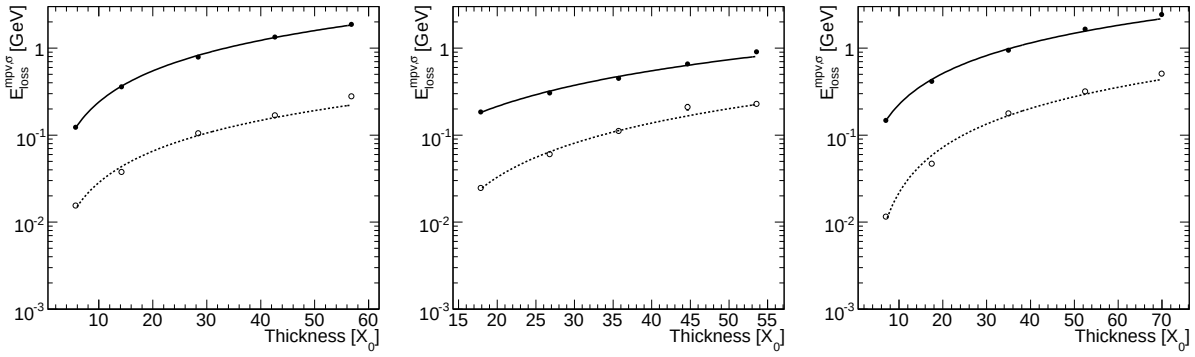

Figure 3: Parameterization of the Landau distribution parameters as a function of thickness of material traversed for 1 TeV muons in iron (left), lead (center) and copper (right). The fitting functions were $a_0x + a_1x\ln(x/X_0)$. The solid (empty) circles and solid (dashed) line correspond to the data and fitted functions for $E_{\rm loss}^{\rm mpv}$ ($E_{\rm loss}^{\sigma}$).

where the constant term corresponds to ionization, the logarithmic term to the relativistic rise (with B=1 GeV^{-1}) and the linear term to the radiative part [6]. These fits are shown in Figure 4. The values of the $b_{i,j}$ parameters are shown in Table 1. Note that all the $b_{0,2}$ parameters are less than 0. This implies that the radiative contribution to the energy loss, $(b_{0,2}x + b_{1,2}x\ln x)\,p_\mu$ would become less than 0 for very thin materials ($\lesssim 10X_0$). This is of course not true when the parameterization is applied to the range of momenta and material thicknesses relevant for muon tracking corrections studied in this note.

3.2 Scaling of Parameters for the Active Media

In the previous section we have shown parameterizations of the energy loss in the absorber materials of the calorimeters. These parameterizations by themselves cannot model the true energy loss corrections in the ATLAS Calorimeters, since there is also energy lost in the active media. This effect can be as big

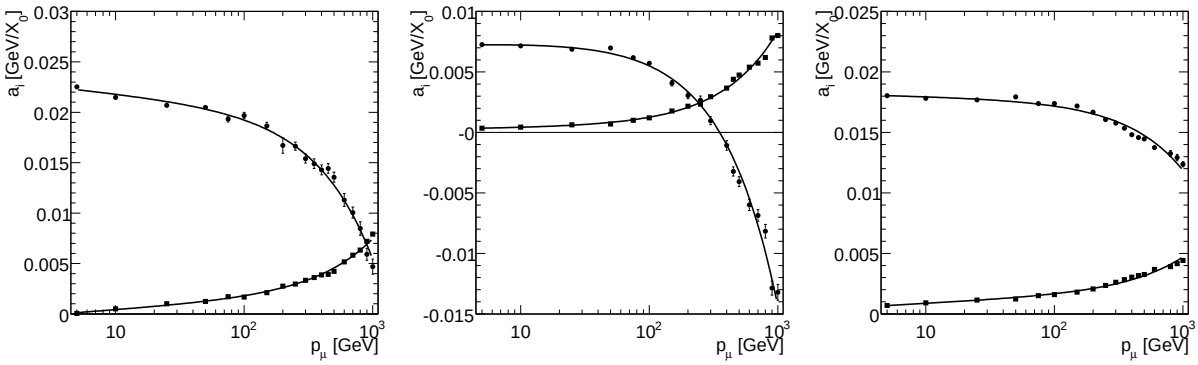

Figure 4: Fit to the a_i parameters (a_0, circles; a_1 squares) for $E_{\text{loss}}^{\text{mpv}}$ as a function of muon momentum in iron (left), lead (center) and copper (right).

		$b_{0,0}$	$b_{0,1}$	$b_{0,2}$	$b_{1,0}$	$b_{1,1}$	$b_{1,2}$
Cu	$E_{\text{loss}}^{\text{mpv}}$	1.82×10^{-2}	-1.1×10^{-4}	-5.6×10^{-6}	2.98×10^{-4}	2.4×10^{-4}	2.77×10^{-6}
	E_{loss}^{σ}	1.18×10^{-3}	-5×10^{-5}	-3.51×10^{-6}	-2.2×10^{-4}	7.4×10^{-5}	1.98×10^{-6}
Fe	$E_{\text{loss}}^{\text{mpv}}$	2.3×10^{-2}	-5.6×10^{-4}	-1.39×10^{-5}	-5.3×10^{-4}	3.9×10^{-4}	5.3×10^{-6}
	E_{loss}^{σ}	1.2×10^{-3}	2.1×10^{-4}	-8.5×10^{-6}	-2.8×10^{-4}	2.4×10^{-5}	3.6×10^{-6}
Pb	$E_{\text{loss}}^{\text{mpv}}$	7.2×10^{-3}	7×10^{-5}	-1.28×10^{-5}	2.2×10^{-4}	8×10^{-5}	4.5×10^{-6}
	E_{loss}^{σ}	6×10^{-4}	-5×10^{-5}	-8.2×10^{-6}	-1.1×10^{-4}	4×10^{-5}	3.01×10^{-6}

Table 1: Fit values of the different parameters for the two parameters of the Landau distribution of the energy loss for the three materials chosen. $b_{i,0}$ and $b_{i,1}$ ($b_{i,2}$) are expressed in GeV X_0^{-1} (X_0^{-1}).

as 30% for the EM calorimeters. For this reason, the most probable value needs to be corrected:

$$E_{\text{loss,calo}}^{\text{mpv}} = E_{\text{loss,param}}^{\text{mpv}} \frac{E_{\text{loss,absorb}}^{\text{mpv}} + E_{\text{loss,active}}^{\text{mpv}}}{E_{\text{loss,absorb}}^{\text{mpv}}} = E_{\text{loss,param}}^{\text{mpv}} \left(\frac{1}{1 - f_{\text{sampl}}} \right). \tag{2}$$

In Equation 2, $E_{\text{loss,param}}^{\text{mpv}}$ is the parameterized most probable energy loss (in the absorber material, from Section 3.1), $E_{\text{loss,absorb}}^{\text{mpv}}$ is the most probable energy lost in the absorber material of the calorimeter, and $E_{\text{loss,active}}^{\text{mpv}}$ is the most probable energy lost in the active material of the calorimeters. Then, f_{sampl} is defined as:

$$f_{\text{sampl}} = \frac{E_{\text{loss,active}}^{\text{mpv}}}{E_{\text{loss,absorb}}^{\text{mpv}} + E_{\text{loss,active}}^{\text{mpv}}}. \tag{3}$$

The sampling fractions used for the EM barrel calorimeter and the TileCal were obtained from [7] and [8], respectively. An extra factor was added to the EM calorimeter sampling fraction to account for the e/μ factor (since the sampling fraction in [7] was calculated for electrons). The sampling fraction for the HEC was estimated from the energy loss of minimum ionizing particles (mips) in the copper absorber and the liquid argon active medium [1]. This estimate is valid for low to mid energy muons ($\lesssim 100$ GeV) because they can be approximated as mips. For higher energy muons such a calculation would overestimate the most probable value of the energy loss by 0.1%, which is negligible for the purpose of this parameterization. Finally, the sampling fraction in the EM Endcap Calorimeter requires

a special treatment due to its complex geometry. A parameterization as a function of η was used. This parameterization is shown in Figure 5.

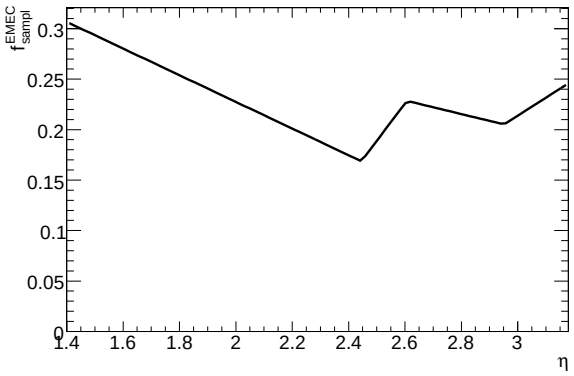

Figure 5: Sampling fraction as a function of η in the ATLAS Endcap EM Calorimeter.

The previous discussion tells how to correct the most probable value of the energy loss distribution, but not the width parameter. There is no comparable well studied quantity like the sampling fraction that can be used to help perform this correction. For this reason, the width parameter was corrected to match the GEANT4 simulation during the validation process. However, this correction turned out to have a non-negligible dependence on the momentum which is difficult to model[1)]. Consequently, the uncertainty in the estimate of the width is much larger than the uncertainty in the estimate of most probable value. See Section 4 for further discussion.

3.3 Energy Loss in Dead Material

Energy lost in dead material also needs to be taken into account. Fortunately, most of the dead material is relatively thin, so only ionization energy loss contributes significantly. Ionization energy loss is well described by a Landau distribution and an analytic calculation of its most probable value exists [9]:

$$E_{\text{loss}}^{\text{mpv}} = \xi \left[\ln \frac{2mc^2}{I} + \ln \frac{\xi}{I} + 3.647 \right], \tag{4}$$

where $\xi = N_A \frac{Z}{A} \frac{k}{\beta^2} x$, where x is the thicknesss of the traversed material in g cm^{-2}, I is the ionization potential of the material, and N_A is Avogadro's number. This approximation is satisfactory for describing the effect for most of the dead material which will be shown in Section 4. However, the support structure of the TileCal, the girder, is over 10 X_0 thick, and therefore the energy lost at this point does not obey Equation 4.

3.4 Adding Energy Loss Incrementally to the Parameterization of the Track

The estimated energy loss is typically approximated by a gaussian and added to the parameterization of the track. The gaussian approximation and the update of the track are discussed in [4]. The gaussian approximation needs to be done in each volume and, ultimately, each surface. However, one must be

[1)] The width of the Landau distribution represents the magnitude of the fluctuations around the most probable value. This magnitude depends on the characteristics of the active material and its response to muons more strongly than the mpv. This response is different at different muon momenta. Therefore this parameter in a complex material like the instrumented regions of the calorimeter cannot be easily modeled starting from parameterizations of these distributions in the absorber materials only.

careful of an assumption that can affect significantly the total energy loss estimation, namely that the most probable value of a Landau distribution is linear under convolution. In other words, if we assume a gaussian in each volume, the total energy loss will be:

$$E_{\text{loss}}^{\text{mpv}} = \sum_{\text{volumes}} E_{\text{loss},i}^{\text{mpv}} \tag{5}$$

$$E_{\text{loss}}^{\sigma} = \sqrt{\sum_{\text{volumes}} \left(E_{\text{loss},i}^{\sigma}\right)^2}. \tag{6}$$

However, in reality for two Landau distributions [10]:

$$E_{\text{loss},1+2}^{\text{mpv}} = E_{\text{loss},1}^{\text{mpv}} + E_{\text{loss},2}^{\text{mpv}} + E_{\text{loss},1}^{\sigma} \ln\left(1 + \frac{E_{\text{loss},2}^{\sigma}}{E_{\text{loss},1}^{\sigma}}\right) + E_{\text{loss},2}^{\sigma} \ln\left(1 + \frac{E_{\text{loss},1}^{\sigma}}{E_{\text{loss},2}^{\sigma}}\right) \tag{7}$$

$$E_{\text{loss},1+2}^{\sigma} = E_{\text{loss},1}^{\sigma} + E_{\text{loss},2}^{\sigma}. \tag{8}$$

This implies that applying the gaussian assumption at each surface underestimates both total $E_{\text{loss}}^{\text{mpv}}$ and E_{loss}^{σ}. However, the track can be appropriately updated if the track propagation algorithm uses the energy loss information along the trajectory before reaching each surface. This information has been made available to the `Extrapolator` and can be configured in the job steering. Incidentally, this implies that uncertainties in the parameterization of the width translate into uncertainties in the estimate of the most probable energy loss. However, this effect is only noticeable when E_{loss}^{σ} is not small compared to $E_{\text{loss}}^{\text{mpv}}$, namely for high momenta.

4 Validation of the New Parameterization

This section shows the validation of the new parameterization for 10 GeV, 100 GeV and 1 TeV muons. The validation was performed through a direct comparison between the ATLAS GEANT4 full simulation and the energy loss estimate in the Tracking Geometry. The validation algorithm is described and then the results are shown and discussed.

4.1 Algorithm

In order to validate the parameterization for a representative set of extrapolations inside the detector, a custom `G4UserAction` was attached to the GEANT4 simulation. This type of class saves the kinematic variables of the simulated muons in a root ntuple after each interaction with the material. An algorithm was developed to read the root ntuple and create a track with the same kinematic variables as those of the original muon in each event. The track is then extrapolated to different surfaces defined by the user and the energy loss up to this point is saved. The estimated width parameter is also saved. The surfaces used for the studies shown in the next section were chosen to delimit different interesting volumes of the ATLAS detector:

1. Closed cylinder enclosing the volumes prior to reaching the EM calorimeters (Inner Detector and gaps): radius 1447 mm and half-length 3250 mm.

2. Closed cylinder enclosing all volumes up to the end of the active region of the EM calorimeters: radius 2003.5 mm and half-length 4309 mm.

3. Closed cylinder enclosing all volumes up to the end of the active region of the Hadronic calorimeters: radius 3860 mm and half-length 6120 mm.

4. Closed cylinder enclosing all volumes in the Calorimeter Tracking Geometry (including support structures such as the TileCal girder): radius 4250 mm and half-length 6500 mm.

The trajectory of the original muon is also followed to these surfaces, and the muon's energy loss up to each surface is saved. These energy losses are used to fill two distributions of energy loss, the true distribution and the reconstructed distribution in different η bins. The spread in the reconstructed distribution is mostly due to the η binning. The true distributions are fitted to Landau distributions and their most probable values and width parameters are compared to those provided by the reconstruction. The algorithm is available in the ATLAS CVS repository as part of the `TrkDetDescrAlgs` package under the name `EnergyLossValidation` and it was used to produce the results in the next section. The amount of material seen by the muon before reaching each of these four surfaces is shown in Figure 6 in units of X_0 and g cm^{-2}. The amount of material in g cm^{-2} (X_0) is proportional to the ionization (radiative)

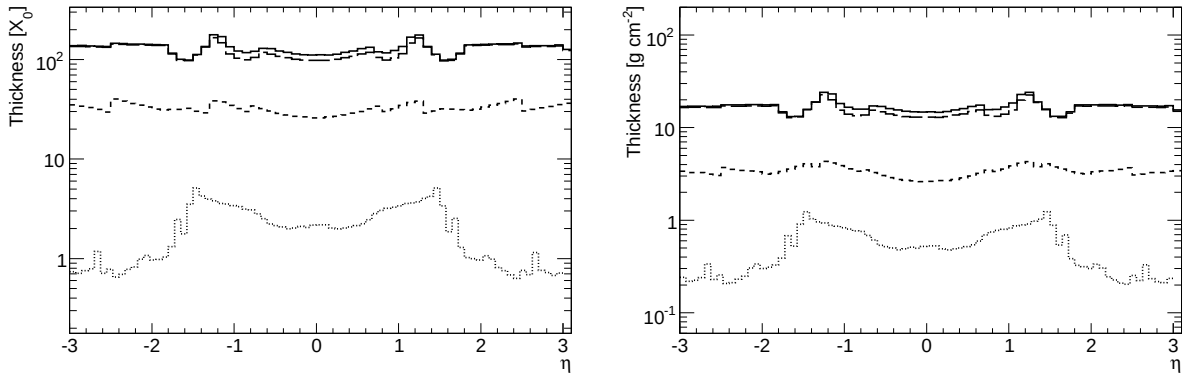

Figure 6: Amount of material traversed by a muon traveling from the interaction point to surface 1 (dotted line), surface 2 (short-dashed line) surface 3 (long-dashed line) and surface 4 (solid line). The thickness is shown in radiation lengths (left) and g cm^{-2} (right).

energy loss. Radiative energy loss grows more rapidly than ionization energy loss in the calorimeters.

4.2 Results

The results obtained with the algorithm just described are summarized in Figures 7 and 8. The error bars on the parameters fit to the simulation (histograms) are not shown. They are ≈10% for $E_{\rm loss}^{\rm mpv}$ and $E_{\rm loss}^{\sigma}$ on average. For the cracks and regions of transition between calorimeters ($|\eta| \approx 1.2$) these uncertainties are larger, since the energy loss distributions are a superposition of several Landau distributions due to the binning in η.

The top left plots correspond to muon trajectories from the beam-pipe to surface 1. The agreement between the most probable energy loss calculated with the simulation and the reconstruction geometry is remarkable; and, in addition, there are no significant differences in the energy loss parameters for 10 GeV and 1 TeV muons. This agreement confirms our assumption that ionization processes describe accurately the energy loss in thin materials.

The top right plots correspond to muon trajectories from the beam-pipe to surface 2. Again in this case, the agreement between simulation and reconstruction is remarkable, even though for specific η regions $E_{\rm loss}^{\sigma}$ seems to be underestimated by as much as 30%. The estimation remains good to an overall 10% accuracy on average.

The bottom left plots correspond to muon trajectories from the beam-pipe to surface 3. The agreement between simulation and reconstruction is also fine for the 10 GeV and the 100 GeV samples. A

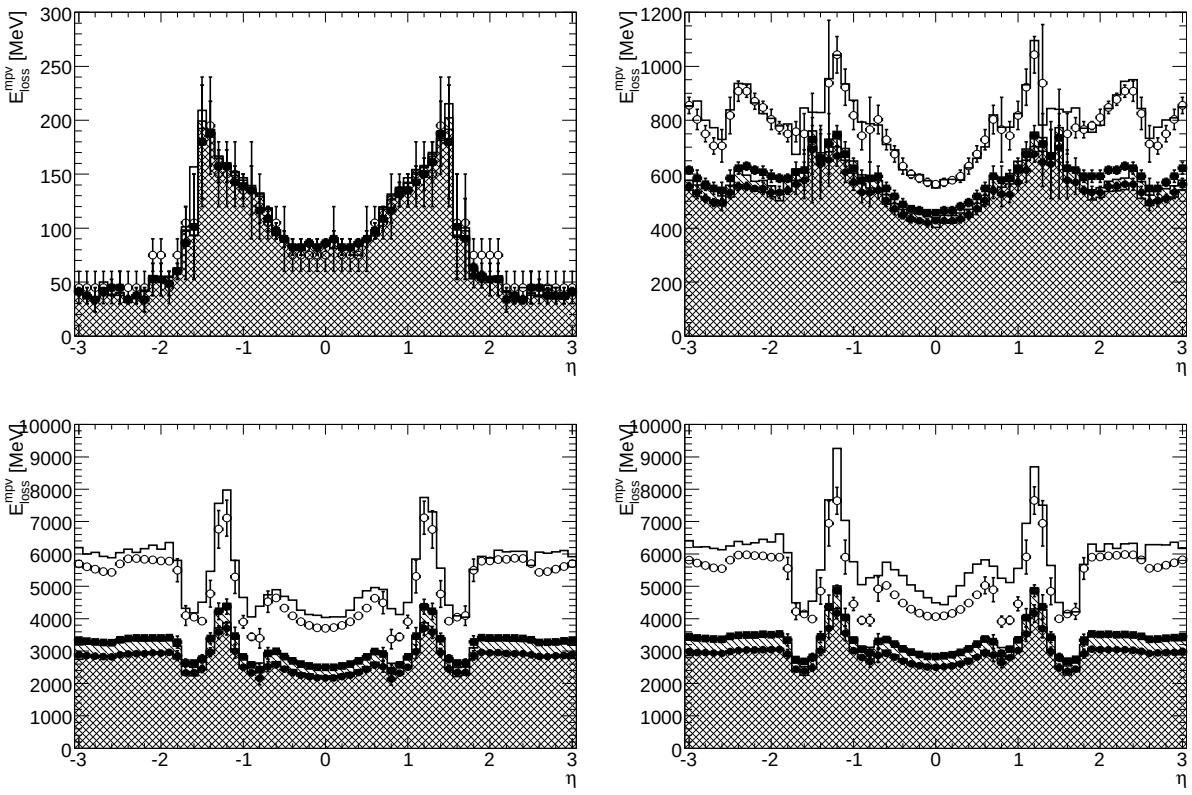

Figure 7: True (histograms) and estimated (points) $E_{\text{loss}}^{\text{mpv}}$ for different muon momenta as a function of pseudorapidity, η. The mpv is calculated for muons propagating from the beam-pipe to 4 different cylinders around the beam pipe in the ATLAS geometry. From left to right and top to bottom: up to the entrance of the EM calorimeters; up to the exit of the EM calorimeters; up to the exit of the hadronic calorimeters; and up to the end of the Tracking Geometry. The double-hatched histogram and solid circles correspond to 10 GeV muons. The single-hatched histogram and solid squares correspond to 100 GeV muons. The empty histogram and empty circles correspond to 1 TeV muons.

small discrepancy of $\approx 5\%$ can be seen for the 1 TeV sample. The underestimation in $E_{\text{loss}}^{\text{mpv}}$ is believed to be correlated to the underestimation in E_{loss}^{σ} seen in Figure 8. A somewhat more important disagreement in the energy loss is visible at $|\eta| \approx 1$. This is due to the modeling of the ITC region of the Extended Barrel TileCal in the Tracking Geometry. This region is essentially made of the same material as the TileCal, but in the Tracking Geometry it is treated as dead material. Therefore, no radiative effects are calculated at this location. This explains why this effect is most remarkable for the 1 TeV sample.

Finally, the bottom right plots present energy loss results for muon trajectories from the beam-pipe to surface 4. The same features as for the bottom left plots are observed with a larger underestimation for $E_{\text{loss}}^{\text{mpv}}$ in the 1 TeV sample and a similar effect on E_{loss}^{σ} for all three samples. This is expected because the energy loss in the support structures like the TileCal girder and the endcap cryostats are not correctly modeled. The effect on the 10 GeV and 100 GeV sample appears only in E_{loss}^{σ} results, which indicates that $E_{\text{loss}}^{\text{mpv}}$ is well-modeled for low and mid-momentum muons and that the estimate for E_{loss}^{σ} does not have a large effect on the estimate for $E_{\text{loss}}^{\text{mpv}}$ in these samples. This is expected since the E_{loss}^{σ} terms in Equation 7 are negligible if E_{loss}^{σ} is very small compared to $E_{\text{loss}}^{\text{mpv}}$.

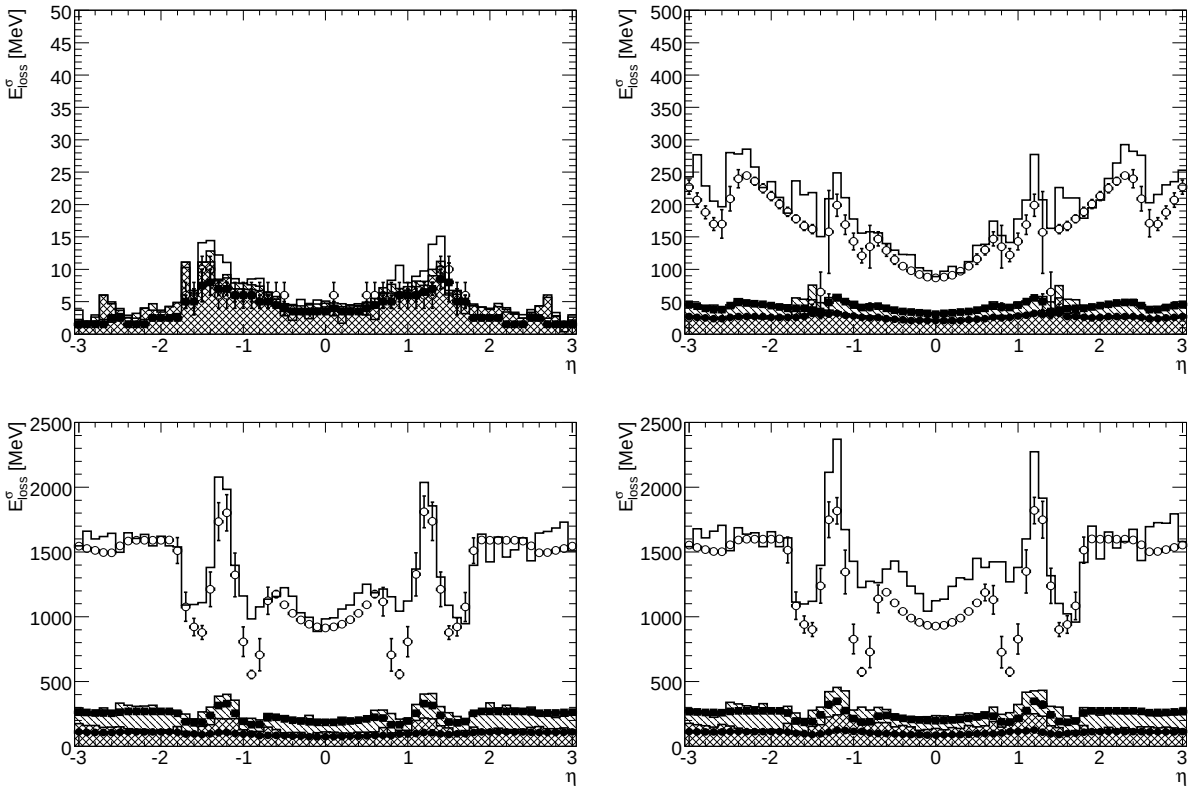

Figure 8: True (histograms) and estimated (points) E^{σ}_{loss} for different muon momenta as a function of pseudorapidity, η. E^{σ}_{loss} is calculated for muons propagating from the beam-pipe to the same 4 different cylinders around the beam pipe as those used for Figure 7.

5 Conclusion

A parameterization of the energy loss of muons in ATLAS has been developed to meet the requirements of the Tracking Geometry. This parameterization is based on analytic calculations of the energy loss and parameterizations of the energy loss in the absorber materials of the calorimeters. The parameterization has been validated in direct comparisons with the GEANT4 full simulation for the variety of extrapolations inside the Tracking Geometry. These validation studies have shown that the parameterization can estimate the most probable value of the Landau distribution of the energy loss accurate to better than 1% on average in the η range from -3 to 3 for 10 GeV and 100 GeV muons. For high momenta muons the parameterization is accurate to $\approx 5\%$ except for extrapolations through the whole Tracking Geometry. For such extrapolations, the TileCal girder contribution to the energy loss is underestimated giving a most probable energy loss of $\approx 10\%$. The estimate for the width parameter in the Landau distribution carries a larger uncertainty for extrapolations through the whole Tracking Geometry, but remains very good for extrapolations inside the calorimeter volumes.

The integration of this parameterization as part of the track extrapolation package for ATLAS provides a reliable transport of muon tracks through the calorimeters. Reliable track transport minimizes biases in the muon momentum estimate for algorithms that reconstruct muon tracks in the Muon Spectrometer. These algorithms are most sensitive to the correct estimate for the energy loss for muons in the few GeV to ≈ 100 GeV momentum range, for which the parameterization presented here has been shown to perform well. The track transport tools expressing the parameterization of the track at the IP allow for

comparisons between different Muon Spectrometer reconstruction algorithms with data, which will be important for evaluating the performance of these algorithms when the first data are collected. Finally, additional algorithms which may require muon energy loss estimates in the calorimeters can also use the `IEnergyLossCalculator` implementing this parameterization.

Appendix: The Landau Distribution and Energy Loss

There is no analytical form for the Landau distribution. The distribution is defined through its Laplace transform

$$\psi(s) = s^s = \exp(s \ln s), \tag{A-1}$$

where s is a complex number. This yields the following form for the Landau distribution:

$$L(x) = \frac{1}{2\pi i} \int_{c-i\infty}^{c+i\infty} e^{sx} \psi(s) ds = \frac{1}{2\pi i} \int_{c-i\infty}^{c+i\infty} \exp(sx + s \ln s) ds. \tag{A-2}$$

The integral is independent of c. This distribution has a well defined most probable value at $x = -0.2228$ and it is characterized by a long tail towards increasing values of x. A generalized form of the Landau distribution can be obtained by performing an affine transformation of Equation A-2. This leads to a Landau distribution with a width parameter a and a scale parameter b:

$$L(x) = \frac{1}{2\pi i} \int_{c-i\infty}^{c+i\infty} e^{sx} \psi(s) ds = \frac{1}{2\pi i} \int_{c-i\infty}^{c+i\infty} \exp[s(x-b) + as \ln(as)] ds. \tag{A-3}$$

When describing energy loss processes by Landau distributions in this document $E_{\text{loss}}^{\text{mpv}} = b - 0.2228$ and $E_{\text{loss}}^{\sigma} = a$. Equations 7 and 8 follow directly [10], since the convolution of any two distributions is the inverse Laplace transform of the product of their Laplace transforms.

The Landau distribution is typically approximated using the CERN library routines [11]. These routines are precise to over 5 significant figures. Throughout this document, fits to Landau distributions were actually fits to the functions defined in the CERN libraries, interfaced through the ROOT standard fitter [12].

Figure A-1 shows the energy loss distributions for muons of different energies going through the ATLAS calorimeters. The distributions were obtained with the ATLAS full simulation, based on GEANT4 [13].

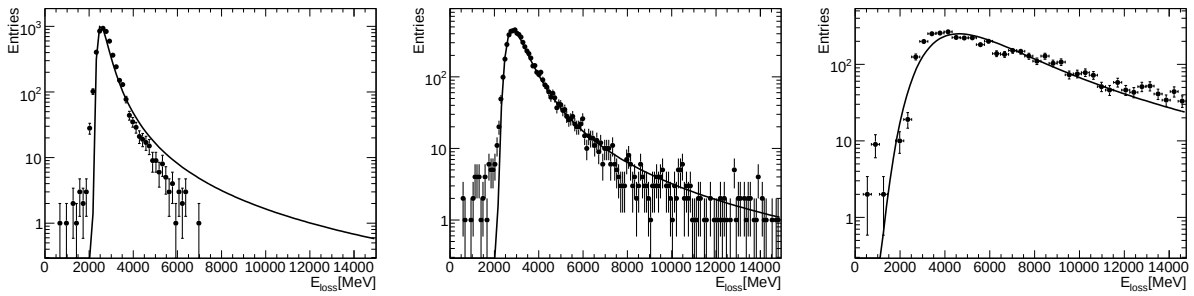

Figure A-1: Energy loss distributions for 10 GeV (left), 100 GeV (center) and 1 TeV (right) muons with $|\eta| < 0.15$ going through the ATLAS calorimeters. Fits to Landau distributions are also shown.

GEANT4 simulates the interactions of muons inside materials. This involves a stepping process, in which the simulated particle is transported without interactions in the material, and an interaction process driven by the cross sections for each type of interaction. The cross sections for electromagnetic

interactions, which cause energy loss of muons, are understood up to $\sim$ 1 TeV [14]. Therefore, the simulation is expected to correctly describe data.

Figure A-1 also shows the Landau distribution fit to each of energy loss distribution. They describe the simulated distributions well, but there are some features that are worth discussing:

- The energy loss distribution for 10 GeV muons is more symmetric than the fit to the Landau distribution.
- The energy loss distribution for 100 GeV muons is well described by the Landau distribution.
- The energy loss distribution for 1 TeV muons deviates from a Landau distribution, having a larger tail. This shifts the most probable value of the fit towards higher values to allow for a better modeling of the tail.

To understand these deviations from the Landau theory, a deeper understanding of the energy loss is needed. Energy loss distributions have been studied in detail [15, 16]. The Landau distribution describes well the fluctuations in ionization energy loss if:

1. The average energy loss is small compared to the maximum energy loss possible in a single muon-electron collision (i.e.: the material is 'thin').
2. The average energy loss is large compared to the binding energy of the most tightly bound electron.

The second condition is always met in the context of this note. It only needs to be considered in gaseous materials, where the average energy loss is very small. If the first condition is not met (in 'thick' materials), the energy loss distribution is described by the Vavilov distributions [16], which tend to be more symmetric than the Landau distribution and approach it in the limit of infinitely thin material. The maximum energy loss possible in a single collision is

$$T_{\max} = \frac{2m_e c^2 \beta^2 \gamma^2}{1 + 2\gamma m_e/m_\mu + (m_e/m_\mu)^2}. \tag{A-4}$$

For a 10 GeV muon, $T_{\max} \sim 3.5$ GeV, which is comparable to the energy lost in calorimeters. For a 100 GeV muon, $T_{\max} \sim 90$ GeV, which is much larger than the average energy lost in calorimeters. $T_{\max}$ grows much faster than the mean ionization energy loss, so for high energy muons the Landau distribution remains appropriate to describe the ionization energy loss distribution. However, radiative energy losses play a more important role as muon energy increases. This implies deviations from the Landau theory, as observed in Figure A-1.

References

[1] W.-M. Yao *et al.,* Journal of Physics G **33** (2006) 1.

[2] T. Cornelissen *et al.,* Concepts, Design and Implementation of the ATLAS New Tracking (NEWT), ATL-SOFT-PUB-2007-007.

[3] A. Salzburger, S. Todorova and M. Wolter, The ATLAS Tracking Geometry Description, ATL-SOFT-PUB-2007-004.

[4] A. Salzburger, The ATLAS Track Extrapolation Package, ATL-SOFT-PUB-2007-005.

[5] D. López Mateos *et al.*, A Bayesian Method for Estimating Energy Loss of Muons in Calorimeters, ATL-COM-MUON-2008-007.

[6] K. Nikolopoulos *et al.*, Muon Energy Loss Upstream of the Muon Spectrometer, ATLAS-MUON-PUB-2007-002.

[7] M. Aleksa *et al.*, 2004 ATLAS Combined Testbeam: Computation and Validation of the Electronic Calibration Constants for the Electromagnetic Calorimeter, ATL-LARG-PUB-2006-003.

[8] G. Schlager, The Energy Response of the ATLAS Calorimeter System, CERN-THESIS-2006-056.

[9] H. Bischel, Rev. Mod. Phys. **60** (1988) 663.

[10] R. Früwirth *et al.*, Data analysis techniques for high-energy physics, p. 293, (Cambridge Univ. Press, Cambridge, second edition, 2000).

[11] K. S. Kölbig and B. Schorr, Comput. Phys. Commun. **31** (1983) 97–111. 21 p.

[12] R. Brun and F. Rademakers, ROOT - An Object Oriented Data Analysis Framework, Proceedings AIHENP'96 Workshop, Lausanne, Sep. 1996, Nucl. Inst. Meth. **A** 389 (1997) 81-86. See also http://root.cern.ch/.

[13] S. Agostinelli *et al.*, Nucl. Instr. and Meth. A **506** (2003) 250.

[14] W. Lohmann, R. Kopp and R. Voss, Energy Loss of Muons in the Energy Range 1-10000 GeV, CERN 85-03 (1985).

[15] L.D. Landau, J. Phys. USSR **8** (1944).

[16] R.V. Vavilov, Zhurn. Exper. i Teor. Fiz. **5** (1957), p. 749.